http://ansinet.com/itj

ITJ

ISSN 1812-5638

INFORMATION TECHNOLOGY JOURNAL

ANSInet
Asian Network for Scientific Information
308 Lasani Town, Sargodha Road, Faisalabad - Pakistan

Information Technology Journal 8 (4): 513-520, 2009
ISSN 1812-5638

Numerical Simulation of Flow Around a Row of Circular Cylinders Using the Lattice Boltzmaim Method

S. Ul Islam and C.Y. Zhou
Harbin Institute of Technology, Shenzhen Graduate School,
Shenzhen University Town, Shenzhen 518055, China

Abstract: This study describes a numerical study of flow past a row of circular cylinders at different Reynolds numbers with different distances between the cylinders using the Lattice Boltzmann Method (LBM). Numerical simulations are performed to investigate the blockage effect for the ranges of $R_e \leq 200$ and $B = W[R] \leq 25R$, where, R_e, R and W are the Reynolds numbers, the radius of the cylinders and the distance between the center of the cylinders, respectively. The Strouhal number and drag forces exerted on the cylinders are quantified jointly with the flow patterns around the cylinders in the form of vorticity contours. It is found that both the drag coefficient and Strouhal number increase when B decreases. It is also observed that the Strouhal number, in general increases as R_e increases for a fixed value of B for the ranges of R_e and B studied. The distance B, between cylinders is limited within 25 in this simulation because of computational resources.

Key words: Lattice Boltzmann method, blockage effect, drag coefficient, strouhal numbers, row of circular cylinders

INTRODUCTION

The flow past a row of circular cylinders is an area of considerable interest to numerical analyst as well as theoreticians. A vast body of knowledge encompassing analytical, numerical and experimental studies is now available on the flow past a circular cylinder (Zdravkovich, 2003). This study will shed light between the drag, blockage ratio (distances between centers of cylinders), Reynolds number and the Strouhal numbers for the two-dimensional flow past a row of circular cylinder. Systematically studied for large distances between centers of the cylinders was conducted by Fornberg (1991).

Over the past few decades, much theoretical and numerical effort has been made to investigate the distances between centers of cylinders (Boppana and Gajjar, 2007; Gajjar and Nabila, 2004; Fornberg, 1998; Natarajan *et al*., 1993; Smith, 1992). Gajjar investigated instability of flow past a cascade of circular cylinders (Gajjar, 2006).

The interface effect between the cylinders in the row is a very remarkable at low Reynolds numbers (Tamada and Fujikawa, 1957). A steady flow through a uniform cascade of normal flat plates numerically and experimentally studies (Ingham *et al*., 1990). However, the studies, especially on numerical simulations of flow past a row of circular cylinders are still relatively partial. Therefore, the further effort is made in this study to study numerically the flow past a row of circular cylinders. In the present study, the Lattice Boltzmann Method (LBM) is employed to simulate such flows past a row of circular cylinders. LBM is originated from the Lattice Gas Cellular Automata (LGCA) (Frisch *et al*., 1986, 1987). In LGCA, the fictitious particles move along lattices with streaming and collision. However, LGCA suffers some drawbacks such as large statistical noise, unphysical velocity-dependent pressure, non-Galilean invariance and large numerical viscosities. It is the lattice Boltzmann method that overcomes the drawbacks of LGCA. In LBM, the Bhatnagar-Gross-Krook (BGK) (Bhatnagar *et al*., 1954) collision model used in the standard Boltzmann equation is adopted.

In recent years, the Lattice Boltzmann Method (LBM) has received considerable attention as an alternative numerical scheme for simulating a variety of fluid dynamic problems (Chopard and Droz, 1998; Wolf-Gladrow, 2000; Succi, 2001; Benzi *et al*., 1992; Chen and Doolen, 1998). A two-dimensional nine-velocity (D2Q9) LBM model (Xiaoyi and Li-Shi, 1997) has been used in this study.

The purpose of the present study is an attempt to examine the effect of distances between centres of cylinders up to Reynolds number of 200. A little information is available about the effect of distances

Corresponding Author: C.Y. Zhou, Harbin Institute of Technology, Shenzhen Graduate School, Shenzhen University Town, Shenzhen 518055, China Tel: 0086-755-25961297 Fax: 0086-755-26033774

between centers of cylinders on drag and wake characteristics. On the other hand, much information is available on the drag, transition from one regime to another, vortex shedding, etc. The numerical study has been carried out using the Lattice Boltzmann Method (LBM). This study shows the capability of the proposed model and the interface effect between the cylinders in the row is very remarkable at low Reynolds numbers.

LATTICE BOLTZMANN METHOD

A square lattice D2Q9 with unit spacing is used in which each node has eight nearest neighbors connected by eight links (Fig. 1). Since, the details of D2Q9 model are given in detail there (Xiaoyi and Li-Shi, 1997) for incompressible Navier-Stokes (NS) equations independent of the density variation. Some basic features of the proposed LBM alone are presented here. Hence, there are two types of moving particles. Particles move along the axis with speed $|e_i| = 1$, i = 1,2,3,4, particles move along the diagonal directions with speed

$$\left|e_i\right| = \sqrt{2}, i = 5,6,7,8$$

Rest particles also allowed at each node with speed zero. The velocity directions of these particles are defined as:

$$e_i = \begin{cases} (0,0), & i=0 \\ \left(\cos\left[\frac{(i-1)\pi}{2}\right], \sin\left[\frac{(i-1)\pi}{2}\right]\right)c, & i=1,2,3,4 \\ \left(\cos\left[\frac{(i-1)\pi}{2}+\frac{\pi}{4}\right], \sin\left[\frac{(i-1)\pi}{2}+\frac{\pi}{4}\right]\right)\sqrt{2}c, & i=5,6,7,8 \end{cases} \quad (1)$$

where, $c = \delta x/\delta t$, δx and δt are the lattice constant and the time step size, respectively.

The particle distribution function satisfies the following evaluation equation of the system is:

$$P_i(x+e_i\delta t, t+\delta t) = P_i(x,t)+\Omega_i \quad (2)$$

where, Ω_i is the collision operator representing the rate of change of the particle distribution function due to collision and $P_i(x,t)$ is the density distribution function. The lattice Boltzmann BGK equation (in lattice units) after Bhatnagar-Groos- Krook (BGK) (Bhatnagar *et al*., 1954), with single-time relaxation approximation is:

$$p_i\left(x+e_i\delta t, t+\delta t\right) = P_i\left(x,t\right) - \frac{1}{\tau}\left[p_i\left(x,t\right) - P_i^{(eq)}\left(x,t\right)\right] \quad (3)$$

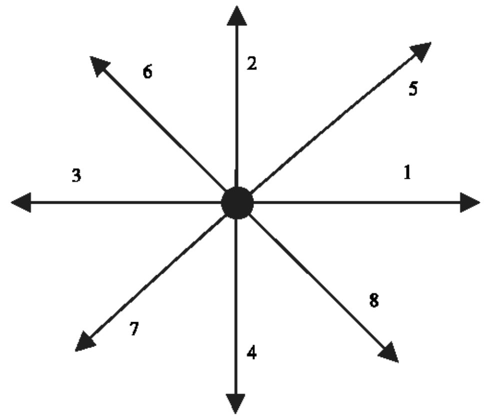

Fig. 1: A two-dimensional nine-velocity lattice (D2Q9) model

where, $P_i^{(e,q)}{}_{(x,t)}$ is the equilibrium pressure distribution at x, t and τ is the relaxation time which controls the rate of approach to equilibrium. The pressure p and the macroscopic velocity u, are defined in terms of the particle distribution function by:

$$p = \sum_i p_i \quad (4)$$

and

$$p_0 u = \sum_i e_i p_i \quad (5)$$

The corresponding equilibrium pressure distribution $P_i^{(eq)}$ defined by:

$$P_i^{(eq)} = w_i\left\{p+\rho_0\left[\frac{3}{c^2}e_i.u+\frac{9}{2c^4}\left(e_i.u\right)^2-\frac{3}{2}\frac{u.u}{c^2}\right]\right\} \quad (6)$$

where, $p = c_S^2\rho$ and ρ_0 is the constant average density. The weighting factor w_i is given by:

$$w_i = \begin{cases} \frac{4}{9}, & i = 0 \\ \frac{1}{9}, & i = 1,2,3,4 \\ \frac{1}{36}, & i = 5,6,7,8 \end{cases} \quad (7)$$

The speed of sound in this model is:

$$c_S = \frac{c}{\sqrt{3}}$$

In order to derive the Navier-Stokes (NS) equations from LBE, under the incompressible flow limit i.e., the Mach number

$$M_a = \frac{|u|}{c_S} << 1$$

the Chapman-Enskog expansion (Chapman *et al*., 1999) is used, in essence with a standard multi-scale expansion proposed by Frisch *et al*. (1987), the mass and momentum equations can be derived from the D_2Q_9 model as follows:

$$\nabla . u = 0 \tag{8}$$

$$\frac{\partial u}{\partial t} + (u.\nabla)u = -\nabla p + \nu \nabla^2 u \tag{9}$$

where, the kinematic viscosity, υ, is:

$$\upsilon = \frac{(2\tau - 1)}{6} \frac{\delta_x^2}{\delta t} \tag{10}$$

Since, the details of this model are given by Xiaoyi and Li-Shi (1997).

PROBLEM STATEMENT AND FORMULATION

The computational domain is drawn in Fig. 2. A two-dimensional flow past a row of circular cylinders with radius R is investigated, where five different values of B= W[R], i.e., 8R,10R,15R,20R and 25R are examined. A rectangular computational domain of B×68R (width×length) is selected with one cylinder lying on the horizontal central line and symmetric boundary condition is applied at the top and bottom boundaries of the computational domain to represent a row of cylinders. Five different lattices 60×504,74×504,112×504,148×504 and 168×504 are used for the five values of B, respectively. The relaxation parameter τ is set to be 0.5173, 0.5086 and 0.5043, respectively.

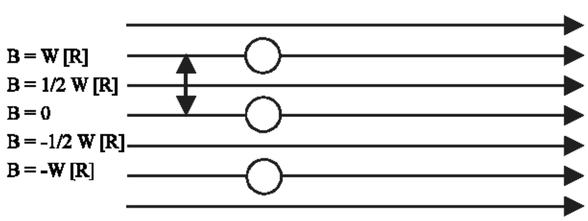

Fig. 2: Schematic flow configuration

BOUNDARY CONDITIONS

Initial condition: Potential flow solution is adopted as an initial condition.

Inlet boundary: A constant pressure gradient along the x-direction is imposed (Luo, 1998):

$$\tilde{f}_i(x,t) = \tilde{f}_i(x,t) - w_i \frac{3}{c^2} \frac{dp}{dx} e_i . \vec{x} \tag{11}$$

where, $\tilde{f}_i$ and $\vec{x}$ are post-collision of distribution function and unit vector along the x axis, respectively.

Outlet boundary: A simple extrapolation is adopted for exit.

$$f_i(N_x, j) = 2f_i(N_x\text{-}i, j)\text{-}f_i(N_x\text{-}2, j) \tag{12}$$

where, N_x, is the number of lattices in the x-direction.

Surface of the cylinder: No-slip wall boundary condition is applied to the surface:

$$u = 0; v = 0 \tag{13}$$

and this is realized with a bounce-back boundary treatment.

Top and bottom boundaries: On the top and bottom boundaries symmetry boundary condition is applied by Renwei (1999).

$$\begin{array}{lll} f_0(i,1) = f_0(i,3), & f_1(i,1) = f_1(i,3), & f_2(i,1) = f_4(i,3) \\ f_3(i,1) = f_3(i,3), & f_4(i,1) = f_2(i,3), & f_5(i,1) = f_8(i,3) \\ f_6(i,1) = f_7(i,3), & f_7(i,1) = f_6(i,3), & f_8(i,1) = f_5(i,3) \end{array} \tag{14}$$

Force evaluation: The momentum exchange method proposed by Dazhi *et al.* (2003) was used in the present study for simulating the flow around the circular cylinder. Since, the details of this model are given here.

$$F = \sum_{all_x b} \sum_{i=1} e_{\bar{i}} \left[\tilde{f}_i(x_b, t) + \tilde{f}_{\bar{i}}\left(xb + e_{\bar{i}}\, \delta t, t\right) \right] \times \left[1 - w\left(xb + e_{\bar{i}}\right) \right] \frac{\delta x}{\delta t} \tag{15}$$

Reynolds number R_e is defined by:

$$R_e = \frac{U\infty D}{\nu} \tag{16}$$

where, D is the cylinder diameter. Other important dimensionless numbers are the drag coefficient C_d, the lift coefficient C_l, the Strouhal number S_t and blockage ratio B. They are defined by the following formulas:

$$C_d = \frac{F_d}{1/2\rho U_\infty^2 D} \quad (17)$$

$$C_l = \frac{F_l}{1/2\rho U_\infty^2 D} \quad (18)$$

$$S_t = \frac{f_s D}{U\infty} \quad (19)$$

$$B = W[R] \quad (20)$$

where, f_s is the vortex shedding frequency from the cylinder, F_d and F_l are the force components in the in-line and transverse directions, respectively.

Computation is terminated when the following convergence criteria is satisfied:

$$\frac{\sqrt{\sum_{l,m}\left[u_{l,m}^{(k=+)} - u_{l,m}^{(k)}\right]^2}}{\sqrt{\sum_{l,m}\left[u_{l,m}^{(k=+)}\right]^2}} \leq 1\times10^{-7} \quad (21)$$

The proposed LBM model (Xiaoyi and Li-Shi, 1997) is independent of density variation. Instead of Eq. 17 and 18 we used Eq. 22 and 23 for calculating drag and lift coefficients (because the density, ρ, is here the average density and is set to be 1.0):

$$C_d = \frac{F_d}{1/2U_\infty^2 D} \quad (22)$$

$$C_l = \frac{F_l}{1/2U_\infty^2 D} \quad (23)$$

RESULTS

The graphical representation of different compositions and comparison with literature data (Fornberg, 1991) shown here. Figure 3 shows how the drag coefficients vary with different blockage ratios.

Figure 4 gives similar behavior for drag coefficient with different Reynolds number (R_e).

The structures of the vorticity filed are shown in Fig. 5a and b.

Figure 6a and b show the vortex formation for different blockage ratios.

The spectrum analysis for the lift coefficient displayed graphically in Fig. 7a-f.

Figure 8-11 show the variation of Strouhal numbers for different blockage ratios, Strouhal number variation for different Reynolds number R_e and similarly examine the effect of drag coefficients for different Reynolds number R_e and blockage ratios.

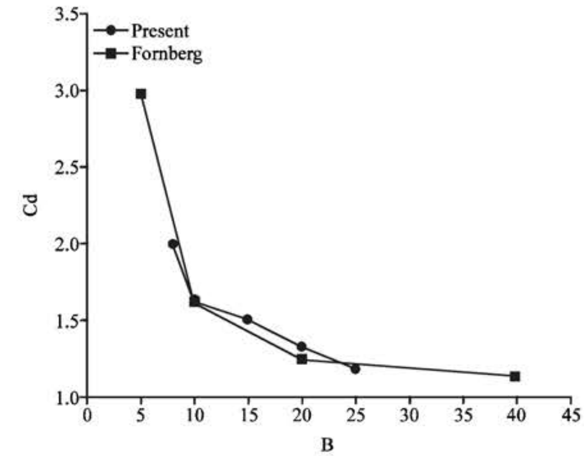

Fig. 3: Variation of drag coefficient with blockage ratios for R_e = 100; line with square box from Fornberg (1991)

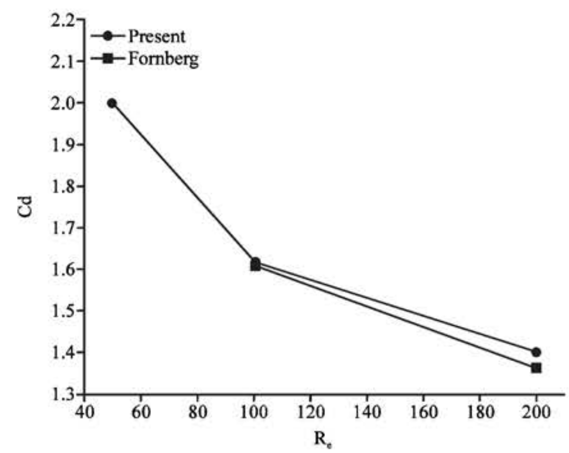

Fig. 4: Variation of drag coefficient with Reynolds number for B = 10; line with square box from Fornberg (1991)

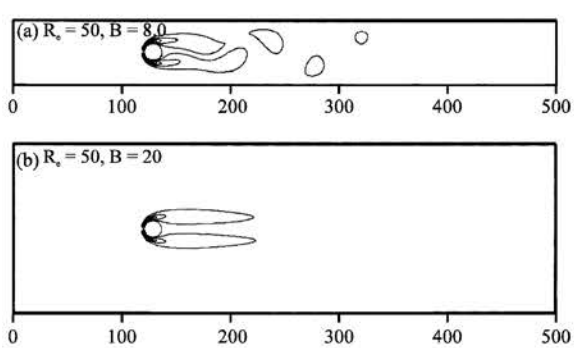

Fig. 5: Vorticity contours of vortex wake of the cylinder for R_e = 50, (a) B = 8 and (b) B = 20

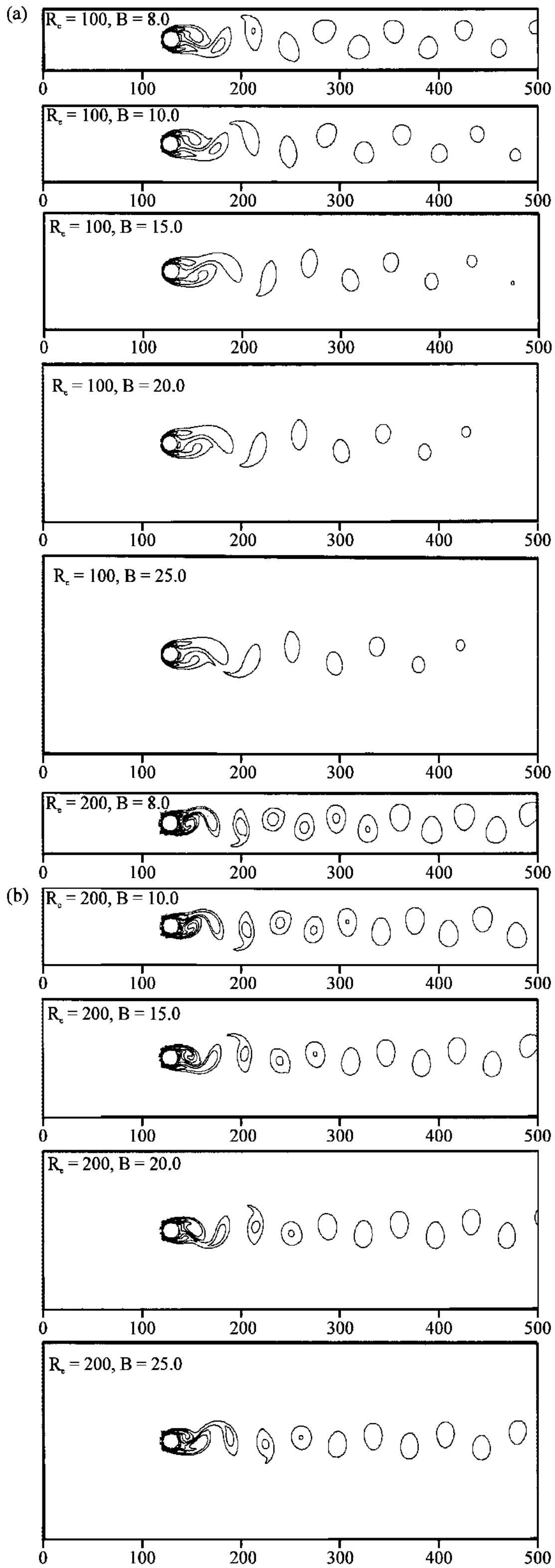

Fig. 6: Vorticity contours of vortex wake of the cylinder for different blockage ratio with (a) R_c = 100 and (b) 200

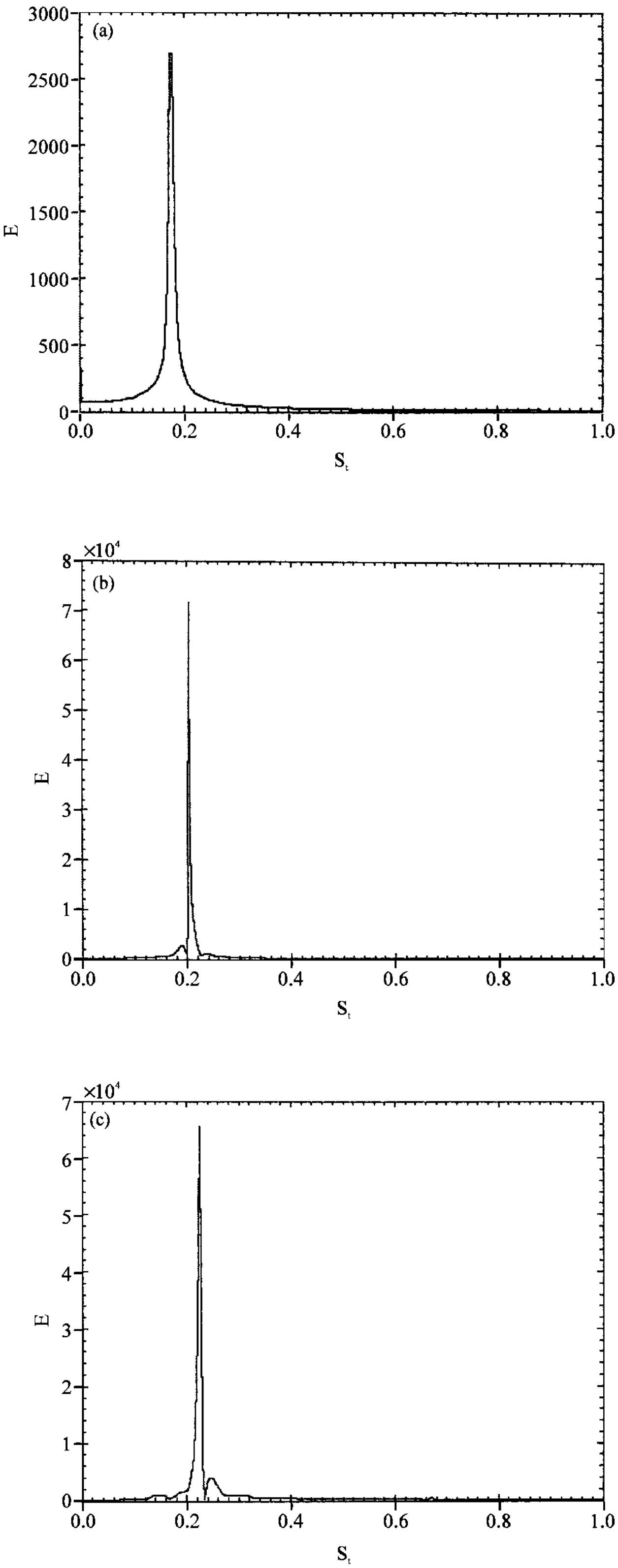

Fig. 7: Continued

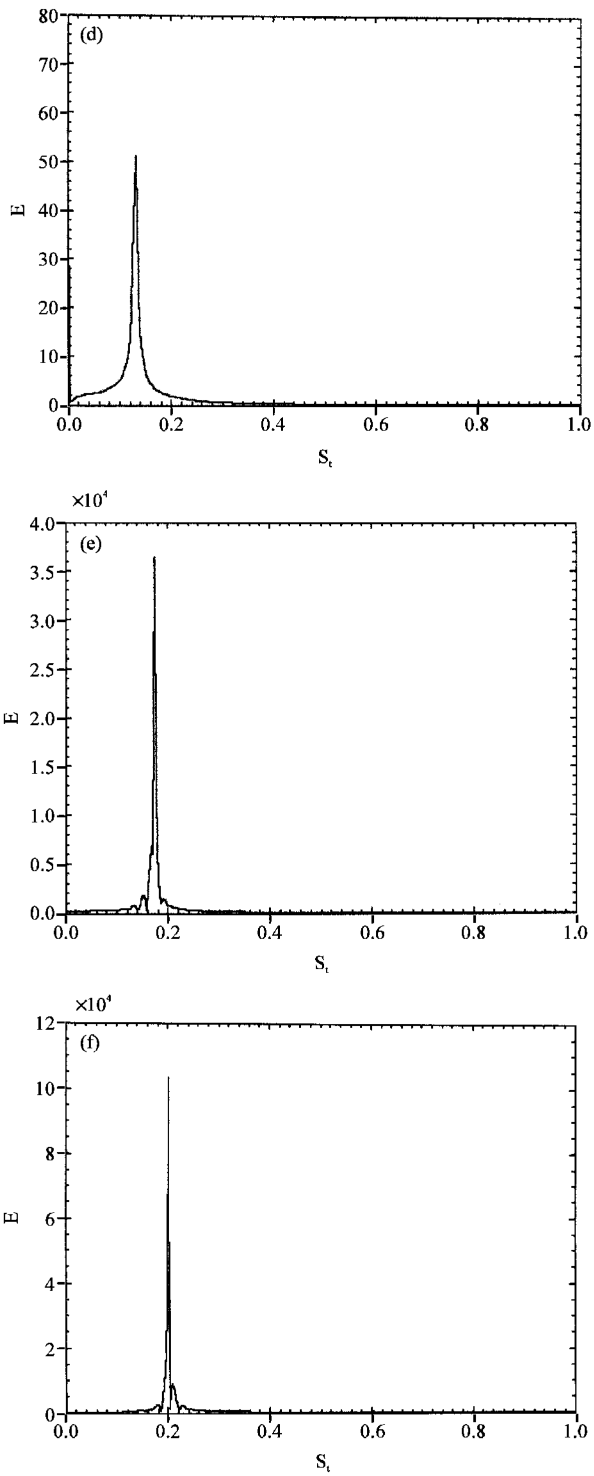

Fig. 7: Spectrum analysis of lift force time history, (a) B = 10, R_e = 50, (b) B = 10, R_e =100, (c) B = 10, R_e = 200, (d) B = 25, R_e = 50, (e) B = 25, R_e = 100 and (f) B = 25, R_e = 200

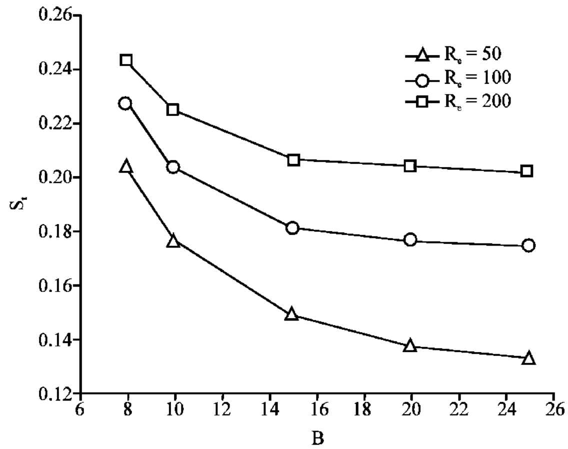

Fig. 8: Variation of S_t with B for different R_e

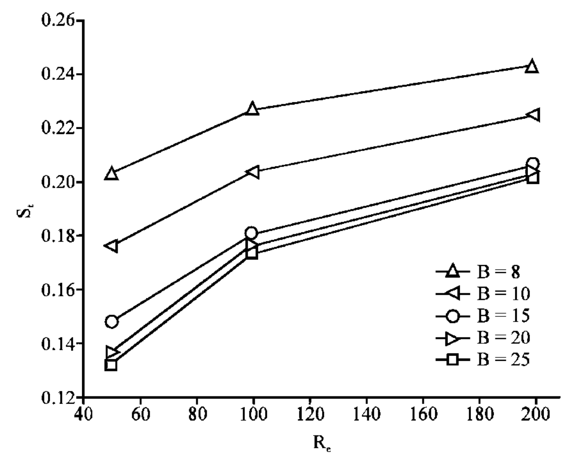

Fig. 9: Variation of S_t with R_e for different B

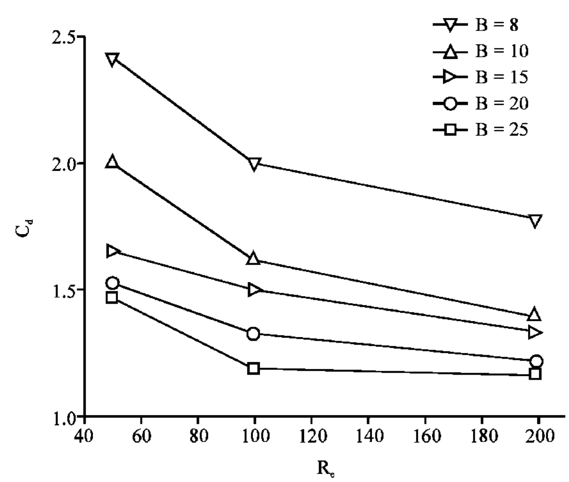

Fig. 10: Variation of C_d with R_e for different B

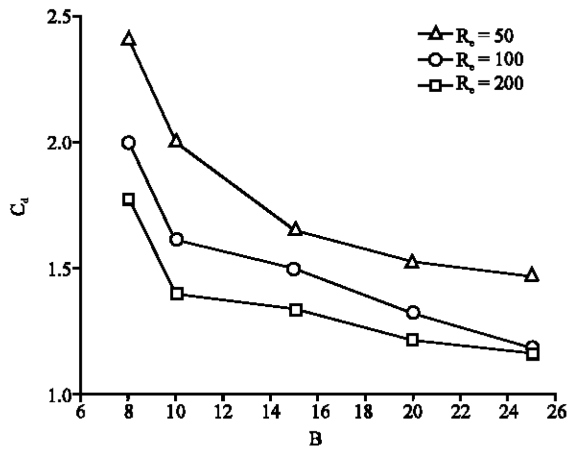

Fig. 11: Variation of C_d with B for different R_e

DISCUSSION

In order to study the effect of the blockage ratio, five blockage ratios, 8, 10, 15, 20 and 25 are investigated for R_e = 50, 100 and 200. The results are compared with some data in literature (Fornberg, 1991). It is seen that the drag coefficient increases as the distance between the cylinders becomes smaller and approaches a steady value as B increases which corresponds to an unbounded flow past an isolated cylinder in Fig. 3. The drag coefficient decreases as R_e increases as expected for this range of the Reynolds number in Fig. 4. For comparison, the numerical results of (Fornberg, 1991) using finite difference method for the same problem are presented in the Fig. 3 and 4 and a good agreement is observed in both figures.

Vortex shedding appears at around R_e = 50. However, vortex shedding starts to appear earlier as the blockage ratio decreases (i.e., as the space between the cylinders becomes smaller) for a fixed Reynolds number. This is shown in Fig. 5. The vortex shedding starts at very early stage during the computation for B = 8 (Fig. 5a), while the wake still maintains a two steady bubbles for a long calculation time for B = 20 (Fig. 5b). This means we not find any disturbance during the whole period of simulations.

Figure 6 the vorticity contours of vortex wake for different blockage ratios are graphically represented. It is seen that both the longitudinal and lateral spacing increase as the blockage ratio increases which is consistent with the observation by Anagnostopoulos and Iliadis (1996).

To study the effect of the blockage on the vortex shedding frequency, the lift force time histories are analyzed using FFT technique for the five blockage ratios. The frequency spectrum analysis results are plotted in Fig. 7 for different blockage ratios.

The results of the spectrum analysis are then shown in Fig. 8 and 9. It can be seen that the vortex shedding frequency decreases as the blockage ratios increases. In other words, the vortices shed with a higher frequency when the distance between the cylinders becomes smaller. The shedding frequency goes up as Reynolds number increases, which shows the general behavior of S_t with R_e for this Reynolds number range. This is similar to an isolated cylinder in a uniform flow as expected. Figure 10 and 11 show that the drag coefficient goes up as Reynolds number decreases and drag coefficient decreases when the blockage ratios increases with fixed Reynolds number.

In practice, the flows past a row of circular cylinders are usually more important and are also hard to incorporate. Therefore, we put more emphasis on them in this study to numerically investigate such types of flows. There is a slight difference with the present and literature data (Fornberg, 1991). Many possibilities are here: different numerical method, limitations of the present method, inflow boundary conditions, side wall boundary conditions and so on.

CONCLUSION

A numerical investigation on a uniform flow past a row of circular cylinders is conducted using the lattice Boltzmann method. The effects of the blockage ratio on the drag coefficient, the vortex wake and vortex shedding frequency are examined. The results show that both the drag coefficient and the vortex shedding frequency increase as the cylinders becomes closer. The present results show good agreement with some data in literature (Fornberg, 1991) and indicate the capability of the LBM in simulating the flow field with complex geometries. This study also sheds the light on the effect of the numerical blockage effect on a numerical solution for an unbounded circular cylinder. When the grids with high blockage are used for reducing the computational time required, the values of the various hydrodynamic parameters may be considerably different from what they should be. When R_e = 50, as B increases, the wake flow becomes steady. However, as B decreases the alternate vortex shedding from the cylinder occurs. The current simulation shows that the proposed method is capable of handling such types of flows problems.

ACKNOWLEDGMENT

The study described in this research was supported by a grant from National Natural Science Foundation of China (Project No. 90715031). The financial support is gratefully acknowledged.

REFRENCES

Anagnostopoulos, P. and G. Iliadis, 1996. Numerical study of the blockage effects on viscous flow past a circular cylinder. Int. J. Numerical Methods Flows, 22: 1061-1074.

Benzi, R., S. Succi and M. Vergasola, 1992. The lattice Boltzmann equation theory and applications. Phys. Rep., 222: 145-197.

Bhatnagar, P.L., E.P. Gross and M. Krook, 1954. A model for collision processes in gases, I. small amplitude processes in charged and neutral one-component system. Phys. Rev., 94: 511-525.

Boppana, V.B.L. and J.S.B. Gajjar, 2007. Stability of flow past cylinder cascade. Proc. Applied Math. Mech., 7: 2100003-2100004.

Chapman, S., T.G. Cowling and D. Burnett, 1970. The Mathematical Theory of Nonuniform Gases. Cambridge University Press, Cambridge, ISBN: 052140844X.

Chen, S. and G.D. Doolen, 1998. Lattice Boltzmann method for fluid flows. Ann. Rev. Fluid Mech., 30: 329-364.

Chopard, B. and M. Droz, 1998. Cellular Automata Modeling of Physical Systems. Cambridge University Press, Cambridge, UK., ISBN: 0 521 46168 5.

Dazhi, Y., M. Renwei, L.S. Luo and S. Wei, 2003. Viscous flow computations with the method of lattice Boltzmann equation. Prog. Aerospace Sci., 39: 329-367.

Fornberg, B., 1991. Steady incompressible flow past a row of circular cylinders. J. Fluid Mech., 225: 655-671.

Fornberg, B., 1998. A numerical study of steady viscous flow past a circular cylinder. Int. J. Numer. Meth. Fluids, 98: 819-855.

Frisch, U., N. Hasslacher and Y. Pomeau, 1986. Lattice-gas automata for the Navier-tokes equations. Phys. Rev. Lett., 56: 1505-1508.

Frisch, U., D. D'humieres, B. Hasslacher, P. Lallemand, Y. Pomeau and J.P. Rivet, 1987. Lattice gas hydrodynamics in two and three dimensions. Complex Syst., 1: 649-707.

Gajjar, S.J.B. and A.A. Nabila, 2004. Numerical solution of the Navier-Stokes equations for the flow in a cylinder cascade. J. Fluid Mech., 520: 51-82.

Gajjar, J.S.B., 2006. Instability of flow past a cascade of circular cylinders. Proceedings of the 6th IUTAM Symposium on Laminar-Turbulent Transition, 2006, Springer Netherlands, pp: 189-194.

Ingham, D.B. T. Tang and B.R. Morton, 1990. Steady two-dimensional flow through a row of normal flat plates. J. Fluid Mech., 210: 281-302.

Luo, L.S., 1998. Unified theory of the lattice Boltzmann models for non-ideal gases. Phys. Rev. Lett., 81: 1618-1626.

Natarajan, R., B. Fornberg and A. Acrivos, 1993. Flow past a row of flat plates at large Reynolds numbers. Proc. R. Soc. Lond., A441: 211-235.

Renwei, M., L. Li-Shi and S. Wei, 1999. An accurate curved boundary treatment in the lattice Boltzmann method. J. Computat. Phys., 155: 307-330.

Smith, F., 1992. Laminar flow of an incompressible fluid past a bluff body: The separation, reattachement, eddy properties and drag. J. Fluid Mech., 92: 171-205.

Succi, S., 2001. The Lattice Boltzmann Equation for Fluid Dynamics and Beyond. Oxford University Press, New York, ISBN: 0 19 850398 9.

Tamada, K. and H. Fujikawa, 1957. The steady two-dimensional flow of viscous fluid at low Reynolds numbers passing through an infinite row of equal parallel circular cylinders. Q. J. Mech. Applied Math., 10: 425-432.

Wolf-Gladrow, DA., 2000. Lattice-Gas Cellular Automata and Lattice Boltzmann Models. An Introduction. Springer, Berlin, ISBN: 3540669736.

Xiaoyi, H. and L. Li-Shi, 1997. Lattice Boltzmann model for the incompressible navier-stokes equation. J. Stat. Phys., 88: 927-944.

Zdravkovich, M.M., 2003. Flow Around Circular Cylinders: A Comprehensive Guide Through Flow Phenomena, Experiments, Applications, Mathematical Models and Computer Simulations. Oxford University Press, New York, ISBN: 0198565615.